4d Orbital Ruthenium Doping Enables High-Capacity and Stable α-MnO_2 Cathodes for Aqueous Zinc-Ion Batteries

Xinyang Zhang [a], Guochao Zhao [a], Xueyan Yang [a], Dewei Wang [a,*], Yuhong Chen [b], Chunping Hou[a]

[a] College of Materials Science and Engineering, North Minzu University, Yinchuan 750021, People's Republic of China. Email: wangdewei@yeah.net (D. Wang)

[b] Ningxia Key Laboratory of Powder Materials Intelligent Design and Manufacturing, North Minzu University, Yinchuan 750021, People's Republic of China.

Computational details

All DFT calculations were performed using the Vienna Ab initio Simulation Package (VASP). The projector augmented-wave (PAW) method was employed to describe electron-ion interactions, while the Perdew-Burke-Ernzerhof (PBE) functional treated exchange-correlation effects. Grimme's DFT-D3 correction was applied to account for van der Waals interactions, and the climbing image nudged elastic band (CI-NEB) method was used to determine minimum energy pathways for ion migration. A plane-wave energy cutoff of 500 eV was adopted throughout the calculations. Structural optimizations and transition state searches were considered convergent when the forces on all atoms were below 0.02 eV/Å and 0.03 eV/Å, respectively. Brillouin zone sampling was performed using 3×3×6 Monkhorst-Pack k-point meshes. Post-processing and visualization were carried out with VASPkit and VESTA, respectively. For band structure calculations and Zn^{2+} migration pathway analysis, the α-MnO_2 unit cell was expanded by a factor of two along the z-direction. The Ru-doped structure was subsequently constructed by replacing one Mn atom with Ru in the resulting supercell.

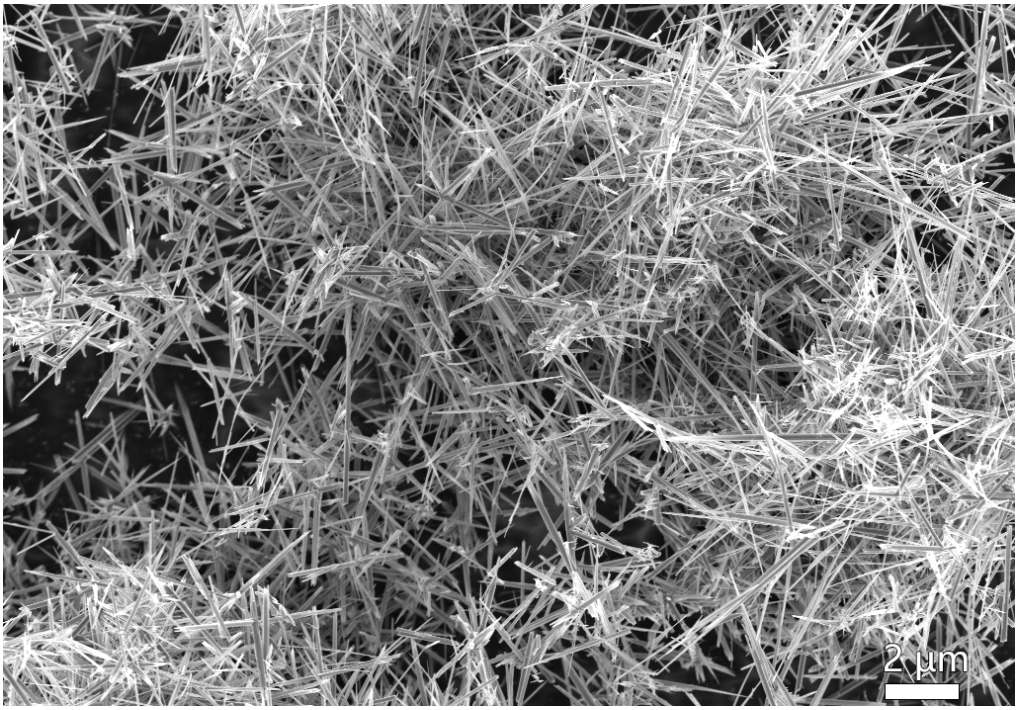

Figure S1. SEM image of RMO at low magnification.

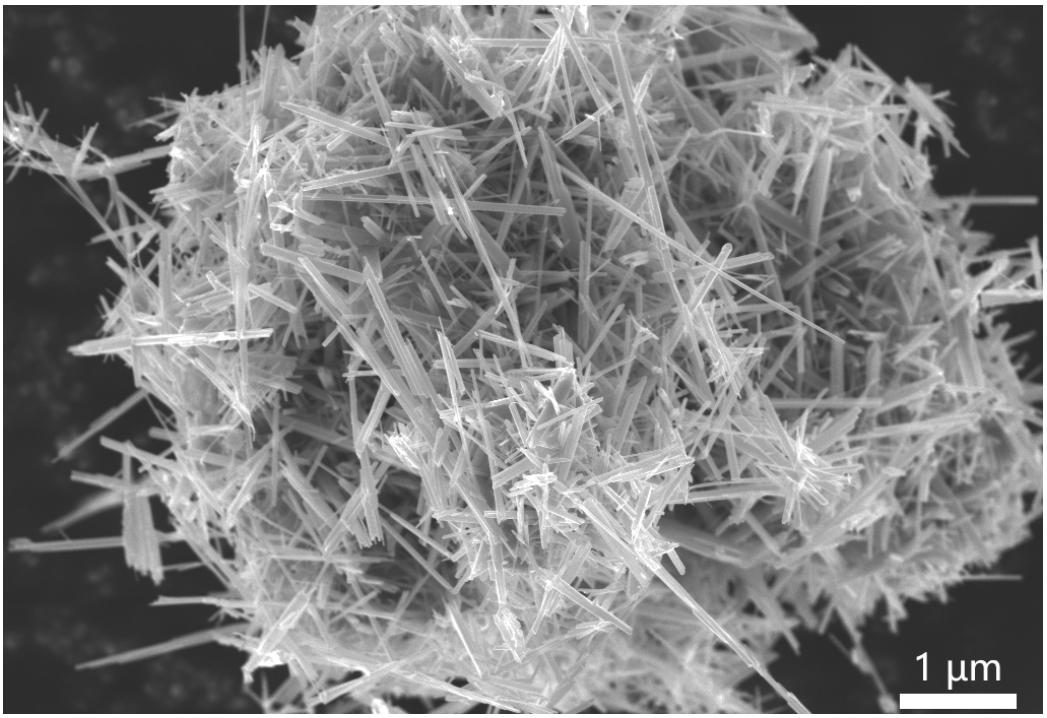

Figure S2. SEM image of PMO.

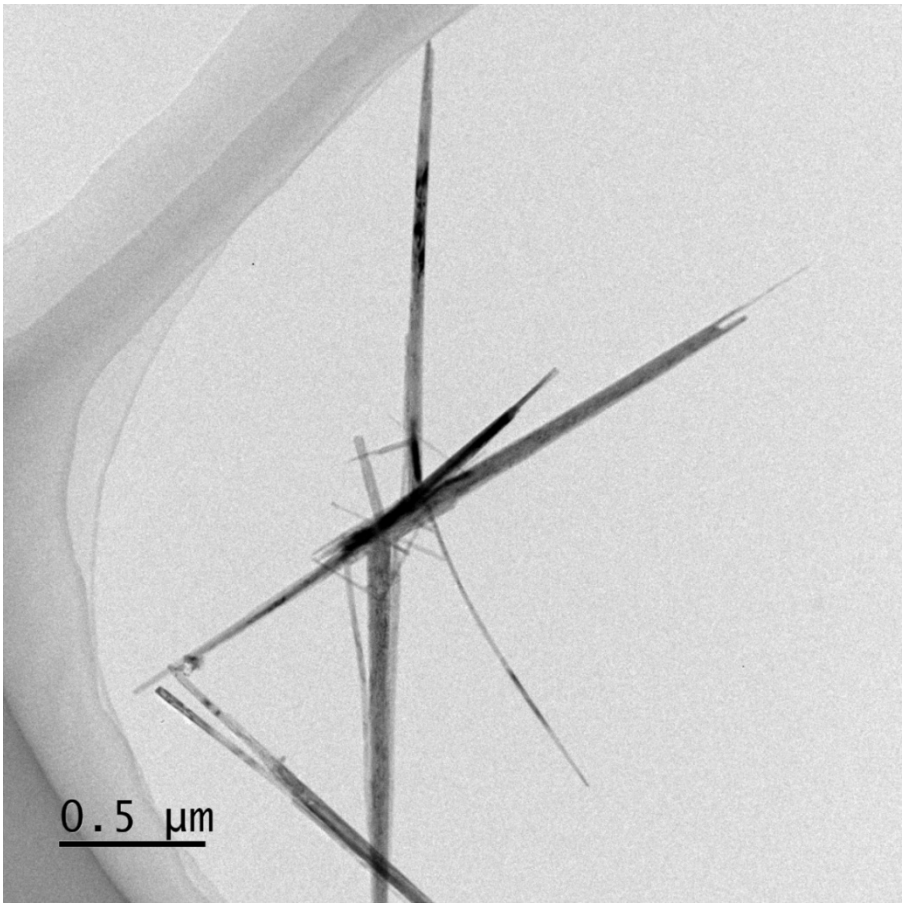

Figure S3. TEM image of RMO at low magnification.

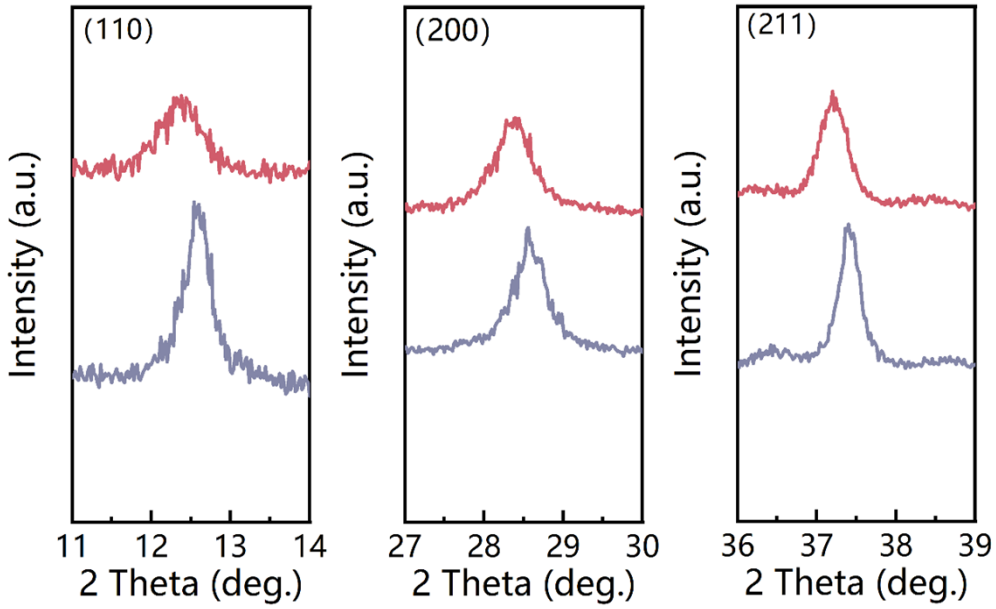

Figure S4. XRD pattern at different lattice plane.

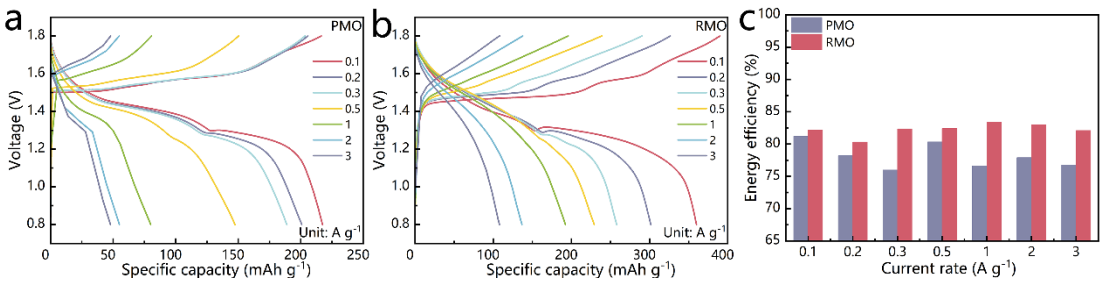

Figure S5. (a) GCD curves of PMO and (b) RMO at different current densities. (c) The corresponding energy efficiency.

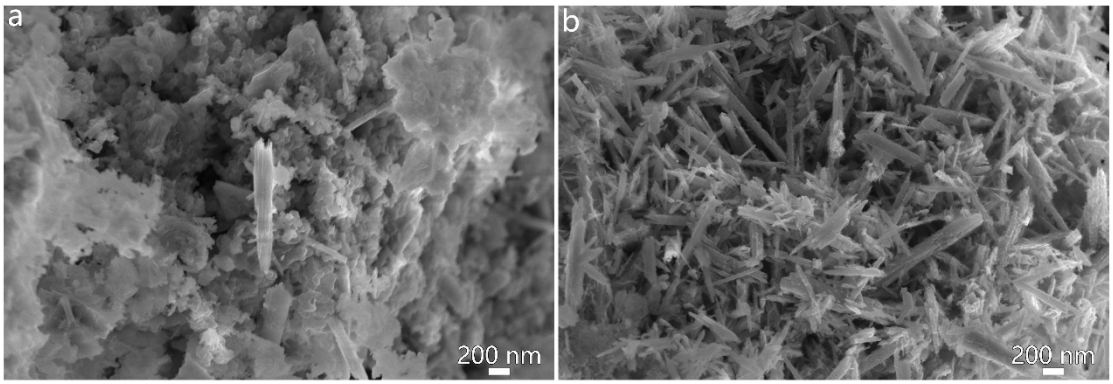

Figure S6. SEM images of the cathodes after cycling. (a) PMO and (b) RMO.

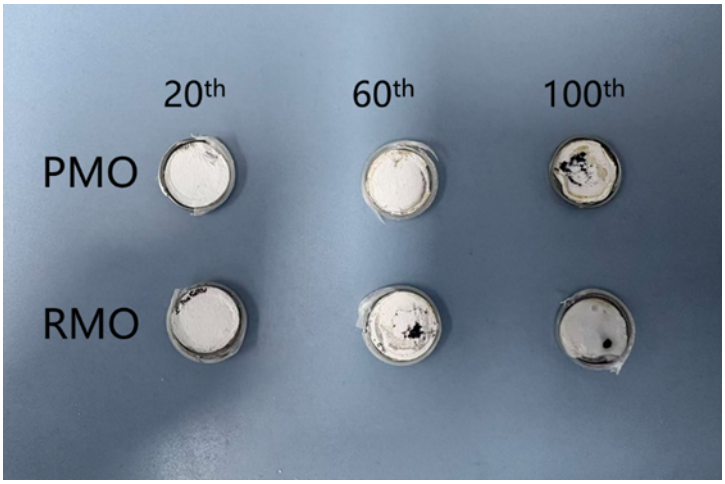

Figure S7. Digital images showing the color evolution of separators after different cycle numbers.

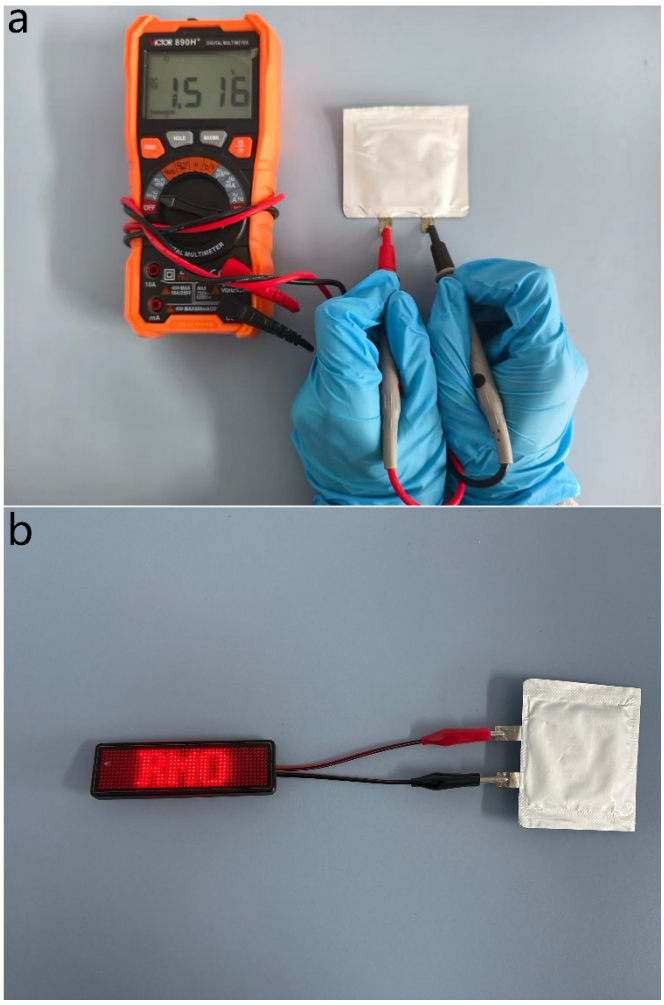

Figure S8. (a) Digital photograph showing the open-circuit voltage of RMO-based pouch cell. (b) Digital photograph of a red light-emitting diode (LED) module (labeled "RMO") powered by the RMO-based pouch cell.

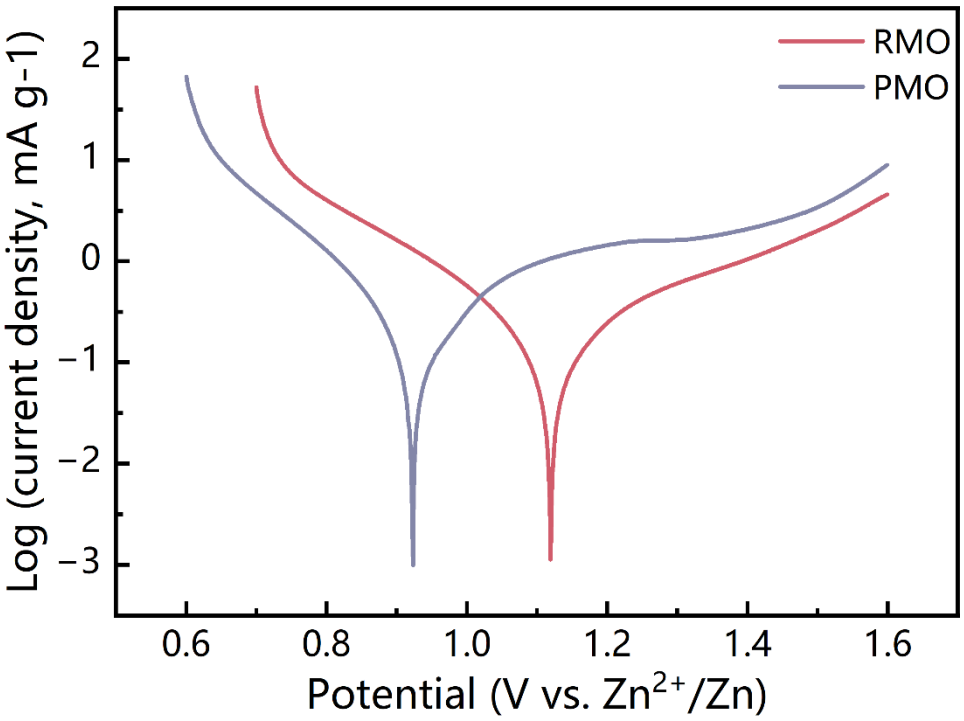

Figure S9. Tafel plots of the PMO and RMO based cathodes.

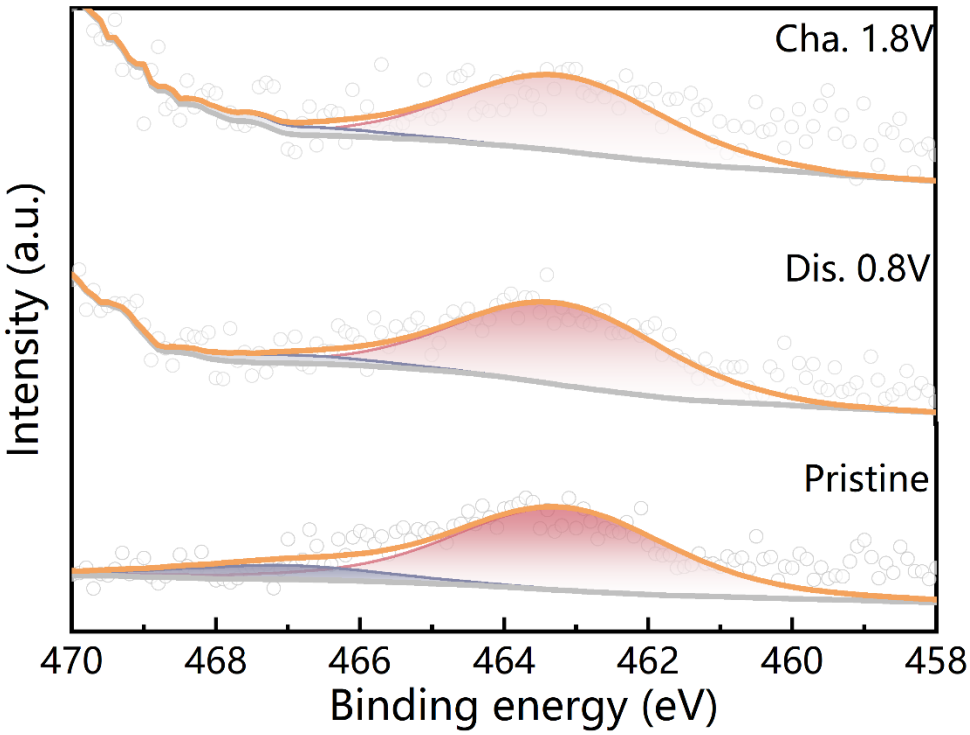

Figure S10. High-resolution XPS spectra of Ru 3p at different states.

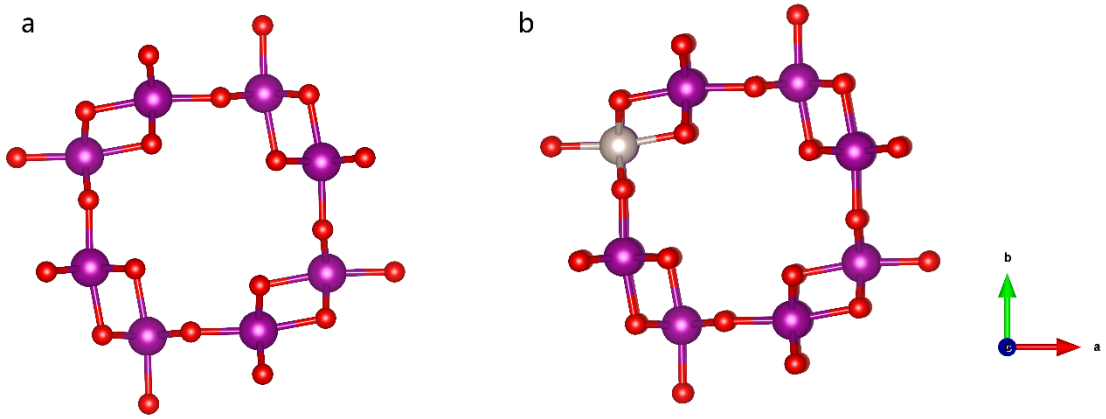

Figure S11. The optimized crystal structure (a) PMO and (b) RMO.

Table S1. Electronegativity and M–O Bond Energy of Transition Metal Elements (Data from J.A. Dean, *Lange's Handbook of Chemistry*, 1999)

Element	Electronegativity	M–O Bond Energy ($kJ \cdot mol^{-1}$)
Ti	1.54	662
V	1.63	541
Cr	1.66	449
Mn	1.55	362
Fe	1.83	407
Co	1.88	424
Ni	1.91	391
Cu	1.90	303
Zn	1.65	280
Mo	2.16	607
Ag	1.93	213
Ru	2.2	626

Table S2. Ionic Radii of Selected Cations and Comparison with Mn^{4+} (Data from J.A. Dean, *Lange's Handbook of Chemistry*, 1999)

Ion	Oxidation State	Ionic Radius (Å)	Difference from Mn^{4+} (Å)
Mn^{4+}	+4	0.53	/
Fe^{3+}	+3	0.64	+0.11
Co^{2+}	+2	0.745	+0.215
Ni^{2+}	+2	0.69	+0.16
Ru^{3+}	+3	0.68	+0.15
Ru^{4+}	+4	0.62	+0.09

Table S3. Comparison of the electrochemical performance of the RMO with recently reported cathodes.

Sample (mass loading)	Specific capacity (mAh g^{-1}) Current density and voltage window	electrolyte composition	Rate capacity retention	Capacity retention	Reference
a-AMO 1 mg cm^{-2}	284.2 at 0.1 A g^{-1} 0.7-1.9 V	2 M $ZnSO_4$ and 0.2 M $MnSO_4$	111 mAh g^{-1} at 3.0 A g^{-1}	60.9% at 1.0 A g^{-1} (after 1000 cycles)	[1]
Cu-MnO_2 1.5 mg cm^{-2}	617.8 at 0.5 A g^{-1} 0.8-1.8 V	2 M $ZnSO_4$ and 0.2 M $MnSO_4$	87.3 mAh g^{-1} at 3 A g^{-1}	93.3% at 1.0 A g^{-1} (after 400 cycles) 54.3% at 5 A g^{-1} (after 1500 cycles)	[2]
Bi-MnO_2 2 mg cm^{-2}	363 at 0.1 A g^{-1} 0.8-1.8 V	2 M $ZnSO_4$ and 0.2 M $MnSO_4$	103 mAh g^{-1} at 3.0 A g^{-1}	100% at 0.1 A g^{-1} (after 100 cycles) 93% at 1.0 A g^{-1} (after 10000 cycles)	[3]
FMO	356.7 at 0.1	2 M $ZnSO_4$	270.2 mAh g^{-1}	88.1% at 1A g^{-1}	[4]

1 mg cm^{-2}	A g^{-1} 0.8-1.8 V	and 0.1 M $MnSO_4$	at 2 A g^{-1}	(after 1000 cycles)	
Ni-MnO_2 1.13 mg cm^{-2}	250 at 0.1 A g^{-1} 0.8-1.8 V	2 M $ZnSO_4$ and 0.2 M $MnSO_4$	75 mAh g^{-1} at 3 A g^{-1}	100% at 1 A g^{-1} (after 600 cycles)	[5]
β-MO-MSC-0.02/PDA-0.06 0.52-0.78 mg cm^{-2}	360 at 0.1 A g^{-1} 0.8-1.8 V	2 M $ZnSO_4$ and 0.2 M $MnSO_4$	120 mAh g^{-1} at 2A g^{-1}	100% at 0.2 A g^{-1} (after 170 cycles) 84.9% at 2 A g^{-1} (after 5000 cycles)	[6]
V-MnO_2/CN 1.2 mg cm^{-2}	352.9 at 0.5 A g^{-1} 0.8-1.8 V	2 M $ZnSO_4$ and 0.2 M $MnSO_4$	153 mAh g^{-1} at 5 A g^{-1}	93% at 0.5 A g^{-1} (after 100 cycles) 83.2% at 1 A g^{-1} (after 1000 cycles)	[7]
NH_4-MnO_2 2 mg cm^{-2}	207 at 0.05 A g^{-1} 0.8-1.8 V	0.3 M Zn triflate	111 mAh g^{-1} at 0.5 A g^{-1}	85% at 0.2 A g^{-1} (after 500 cycles)	[8]
$MnO_2(O_d)$ 1.5 mg cm^{-2}	330.9 at 0.1 A g^{-1} 0.8-1.8 V	2 M $ZnSO_4$ and 0.2 M $MnSO_4$	225 mAh g^{-1} at 2.0 A g^{-1}	88.9% at 1 A g^{-1} (after 800 cycles)	[9]
δ-MnO_2@ 2-ML 1.3-2 mg	309.5 at 0.1 A g^{-1} 0.8-1.8 V	2 M $ZnSO_4$ and 0.2 M $MnSO_4$	137.6 mAh g^{-1} at 1.0A g^{-1}	80% at 1.0A g^{-1} (after 1350 cycles)	[10]

cm^{-2}					
K-MnO_2	245.9	2 M $ZnSO_4$	211.8 mAh g^{-1}	99% at 1.0 C	[11]
1-2 mg cm^{-2}	at 0.2 C	and 0.1 M $MnSO_4$	at 4 C	(after 100 cycles)	
	0.8-1.8 V				
Ca/N-MnO_2//Zn	325 at 0.3 A g^{-1}	2 M $ZnSO_4$ and 0.1 M $MnSO_4$	64.2 mAh g^{-1} at 3 A g^{-1}	70% at 1 A g^{-1} (after 200 cycles)	[12]
1.5 mg cm^{-2}	0.9-1.9 V			70.4% at 3 A g^{-1} (after 1000 cycles)	
PANI-MnO_2	479.9 at 0.1 A g^{-1}	2 M $Zn(CF3SO3)_2$	121.2 mAh g^{-1} at 4.0 A g^{-1}	92.1% at 4.0 A g^{-1} (after 2000 cycles)	[13]
	0.6-1.8 V				
In-δ-MnO_2	420 at 0.1 A g^{-1}	2 M $ZnSO_4$ and 0.2 M $MnSO_4$	170 mAh g^{-1} at 2 A g^{-1}	83.6 % at 2 A g^{-1} (after 1000 cycles)	[14]
	1-1.85 V			90.3% at 0.2 A g^{-1} (after 300 cycles)	
a-MnO_2/Ti_3C_2F	506.6 at 0.1 A g^{-1}	1 M $ZnSO_4$ and 0.5 M $MnSO_4$	8.2 mAh g^{-1} at 2 A g^{-1}	100% at 0.3A g^{-1} (after 120 cycles)	[15]
	0.8-1.9 V				
1-2 mg cm^{-2}					
RMO	360.1 at 0.1 A g^{-1}	2 M $ZnSO_4$ and 0.1 M $MnSO_4$	107.9 mAh g^{-1} at 3 A g^{-1}	100% at 0.1A g^{-1} (after 100 cycles)	This work
1 mg cm^{-2}	0.8-1.8 V			76.7% at 3A g^{-1}	

(after 3000 cycles)

References

1 L. Yang, J. Zhang, X. Zhou and Y. Liu, *J. Alloys Compd.*, 2025, **1012**, 178502.

2 R. Jin, Y. Fang, B. Gao, Y. Wan, Y. Zhou, G. Rui, W. Sun, P. Qiu and W. Luo, *Ind. Chem. Mater.*, 2025, **3**, 87-96.

3 Y. Ma, M. Xu, R. Liu, H. Xiao, Y. Liu, X. Wang, Y. Huang and G. Yuan, *Energy Storage Mater.*, 2022, **48**, 212-222.

4 S. Jiang, S. Tian, S. Zhang, L. Fang, Z. Wang, P. Nie, W. Han, X. Xue, C. Zhao and M. Lu, *ACS Appl. Nano Mater.*, 2024, **7**, 27648-27655.

5 X. Liang, X. Liu, P. Wang, Z. Guo, X. Chen, J. Yao, J. Li, Y. Gan, L. Lv and L. Tao, *J. Power Sources*, 2025, **635**, 236518.

6 S. Li, Y. Zhou, J. Li, Y. Feng, M. Liu, N. Li, H. Liu, X. Meng, J. Zhu and R. Chu, *J. Power Sources*, 2025, **656**, 238093

7 Y. Zhao, Y. Zhang, X. Ma, A. Su, Z. Chen and X. Zhang, *J. Colloid Interface Sci.*, 2025, **703**, 139152.

8 W. Kao-Ian, J. Sangsawang, M. Gopalakrishnan, S. Wannapaiboon, A. Watwiangkham, S. Jungsuttiwong, J. Theerthagiri, M. Y. Choi and S. Kheawhom, *ACS Appl. Mater. Interfaces*, 2024, **16**, 56926-56934.

9 J. Zheng, C. Qin, C. Chen, C. Zhang, P. Shi, X. Chen, Y. Gan, J. Li, J. Yao and X. Liu, *J. Mater. Chem. A*, 2023, **11**, 24311-24320.

10 Y. Ding, K. Zhu, H. Jin, W. Gao, B. Wang, S. Bian, R. He, J. Wang, H. Yang and K. Denis, *Carbon Energy*, 2025, **7**, e70014.

11 Y. Li, X. Liu, T. Ji, M. Zhang, X. Yan, M. Yao, D. Sheng, S. Li, P. Ren and Z. Shen, *Chin. Chem. Lett.*, 2025, **36**, 109551.

12 Y. Xu, G. Zhang, X. Wang, J. Zhang, H. Wen, D. Wang, Y. Yuan, Q. Jiang, H. Qian and Y. Xi, *Adv. Funct. Mater.*, 2025, **35**, 2500137.

13 X. Chen, R. Zhang, H. Zou, L. Li, Q. Zhu and W. Zhang, *Scr. Mater.*, 2024, **241**, 115893.

14 S. Liu, Y. Wang, Z. Zhou, W. Zhang and J. Fan, *Colloids Surf., A*, 2024, **699**, 134688.

15 Y. Song, W. Zhan, Z. Wu, Q. Chen, X. Chen, Z. Liu, J. Du, C. Tao and Q. Zhang, *J. Mater. Chem. A*, 2024, **12**, 16910-16920.